



# Invasive Cribriform Carcinoma of the Breast: Radiologic and Histopathologic Features

Youyeon Kim,<sup>1</sup> Kyu Ran Cho,<sup>1\*</sup> Sung Eun Song,<sup>1</sup> Bo Kyung Seo,<sup>2</sup> Ok Hee Woo,<sup>3</sup> Jeong Hyun Lee,<sup>4</sup> and Sung Bum Cho<sup>1</sup>

<sup>1</sup>Department of Radiology, Korea University Anam Hospital, Seoul, Korea

<sup>2</sup>Department of Radiology, Korea University Ansan Hospital, Ansan, Korea

<sup>3</sup>Department of Radiology, Korea University Guro Hospital, Seoul, Korea

<sup>4</sup>Department of Pathology, Korea University Anam Hospital, Seoul, Korea

\*Corresponding author: Kyu Ran Cho, Department of Radiology, Korea University Anam Hospital, Seoul, Korea. Tel: +82-29205657, Fax: +82-29293796, E-mail: krcho@korea.ac.kr

Received 2016 May 13; Revised 2016 August 03; Accepted 2016 September 03.

## Abstract

**Background:** Invasive cribriform carcinoma (ICC) of the breast is a distinct histologic type of invasive carcinoma that is known to have a relatively favorable prognosis. There is very little information about ICC radiologic findings.

**Objectives:** The purpose of this study is to investigate ICC radiological findings, including those of mammography, sonography, and magnetic resonance imaging (MRI), and histopathological findings.

**Patients and Methods:** Mammography, sonography, and MRI findings of twelve female patients with ICC in our institution were retrospectively reviewed by two radiologists in consensus. Diagnoses were based on surgically resected specimens, and image features were reviewed according to the American college of radiology breast imaging reporting and data system (ACR BI-RADS®) lexicon. Histopathological findings were reviewed by two experienced breast pathologists in consensus.

**Results:** Of the twelve patients, eleven underwent pre-operative mammography, and all underwent pre-operative sonography and MRI. Mammographic findings were mass (n = 8), focal asymmetry (n = 2), or no detectable finding (n = 1). Most masses had irregular shapes, indistinct margins, equal densities to the parenchyma, and no associated calcification. By sonography, all masses were hypochoic with variable shapes. The margins of the tumors were mostly indistinct. Each tumor was depicted as an enhancing mass with an irregular, oval, or round shape on MRI. Usually, the margins were irregular, and enhancement patterns were type III. On histopathologic examinations, most tumors were grade I, and all were luminal subtype A by immunohistochemical study.

**Conclusion:** ICCs of the breast appear as masses with typical features of malignancy using radiologic techniques. The differences in the radiologic features of invasive ductal carcinoma of no special type, which is the most common invasive breast malignancy, and ICCs are that ICCs usually appear without associated calcifications and show rare spiculation.

**Keywords:** Breast Neoplasm, Carcinoma, Mammography, Ultrasonography, Magnetic Resonance Imaging

## 1. Background

Breast cancer is the second most common cancer in the world and the most common cancer among women (1). Breast cancer ranks as the fifth leading cause of death from cancer overall, and it is one of the most frequent causes of cancer death in women (1). The world health organization (WHO) classification of breast tumors was updated in 2012 as the 4th edition, providing updated information on molecular pathology, expression profiling, and molecular classification of breast cancer (2, 3). There are many subtypes of invasive breast carcinoma, including invasive lobular, tubular, cribriform, metaplastic, apocrine, mucinous, papillary, and micropapillary carcinoma as well as

carcinoma with medullary, neuroendocrine, and salivary gland/skin adnexal type features (2, 3). These specific subtypes are defined by their morphologies, but they have also been linked to particular clinical, epidemiological, and molecular features (2, 3). Of those special breast cancer subtypes, tubular carcinoma and invasive cribriform carcinoma are tumors with favorable prognoses and low-grade nuclear features (2-5).

Invasive cribriform carcinoma (ICC) of the breast is a distinct histologic type of invasive carcinoma that was first described by Page et al. in 1983 after reviewing the histology and clinical course of 1003 cases of breast cancer (5). ICC is characterized by a cribriform histologic pattern described as cancer cells invading the stroma in nest-like for-

mations between the ducts and lobules in the majority of the invasive component (2-5). ICC is known to have a relatively favorable prognosis, with a low frequency of nodal metastasis (4-8). To our knowledge, there have been few reports of ICC radiologic features probably due to its low incidence, and there is scant information about ICC radiologic features.

## 2. Objectives

The purpose of this study was to investigate the radiological findings of invasive cribriform carcinoma of the breast, including those of mammography, sonography, and magnetic resonance imaging (MRI), as well as the histopathological findings, such as tumor grade and immunohistochemical study results.

## 3. Patients and Methods

This study was conducted with the approval of the institutional review board. A retrospective review of the pathologic and surgical databases at our institution from January 2008 to April 2015 for patients diagnosed with ICC identified twelve patients (mean age, 45.7 years; age range, 37-66 years). All 12 patients had a pathologic diagnosis of ICC after mastectomy or conserving surgery and pre-operative radiologic study within a month of the pathologic diagnosis. Patients had undergone mammography, sonography, MRI, and 18F-fluorodeoxyglucose (18F-FDG) positron emission tomography-computed tomography (PET-CT) pre-operatively.

### 3.1. Mammography

Craniocaudal and mediolateral oblique views were obtained by mammography, using the Lorad Selenia (Hologic Inc., Bedford, MA, USA). Parenchymal patterns were categorized as one of the following: almost entirely fatty, scattered fibroglandular tissue, heterogeneously dense, and extremely dense. Each mammogram was analyzed for mass lesions, asymmetric densities, architectural distortion, and calcifications. If a definite mass was present, the size, shape, margin, and density were also classified.

### 3.2. Sonography

Sonography was performed using the LOGIQ 9 (GE Healthcare, Milwaukee, WI, USA) with a broad-bandwidth 14 - 5 MHz linear probe. All patients underwent examinations of both breasts and axillary lymph nodes. Each lesion was analyzed for size, echogenicity, shape, orientation, margin, posterior features, vascularity, and associated calcifications. We recorded the maximum tumor diameter as the size of the mass (9).

### 3.3. Magnetic Resonance Imaging (MRI)

MRI was performed using a 3.0-T Scanner (Achieva 3.0T TX; Philips Healthcare, Best, the Netherlands) and a breast coil (MRI devices; InVivo research, Orlando, FL, USA), with the patient in the prone position. Images were acquired in the axial plane with the following sequences: axial, diffusion-weighted, spin-echo single-shot echo-planar-imaging with diffusion-sensitizing gradients (repetition time (TR)/echo time (TE), 5471/72; b values, 0, 600, and 1000 s/mm<sup>2</sup>; image matrix, 96 × 126; field of view [FOV], 320 × 320 mm; section thickness, 3 mm; section gap, 0 mm; three signal acquired; and acquisition time, 80 s); axial, T2-weighted, fat-suppressed, fast spin-echo imaging (TR/TE, 5727/70; flip angle, 90°; field of view [FOV], 581 × 342 mm; image matrix, 620 × 309; section thickness, 3 mm; and section gap, 0 mm); pre- and post-contrast enhanced, axial, T1-weighted three-dimensional (3D) fast spoiled gradient echo sequence (TR/TE, 6/3; flip angle, 0°; FOV, 330 × 340 mm; image matrix, 436 × 436; section thickness, 3 mm; and section gap, 1.5 mm). Fifteen mL of gadodiamide (Omniscan, GE Healthcare, Oslo, Norway) was injected intravenously into an antecubital vein with a power injector (Medrad® Spectris, Indianola, PA, USA) at a rate of 2 mL/s. Imaging was performed before the injection and six times after the injection, occurring immediately and then at intervals of 1 minute. The images post-processing, included the subtraction of unenhanced images from enhanced images and 3D maximum-intensity projections by using the first contrast-enhanced series. The interpretation of enhancement degree and kinetic patterns was performed using computer-aided diagnosis (CAD) stream TM (Merge health care, Chicago, IL, USA). The kinetic curves were analyzed as three types: type I, progressive continuous enhancement; type II, initial uptake followed with delayed plateau; and type III, initial rapid uptake with delayed washout. The size, shape, margin, enhancement pattern, and multiplicity were recorded as well as the associated findings, such as nipple retraction, skin retraction or thickening, hematoma, and pectoralis muscle or chest wall invasion.

All mammographic, sonographic, and MR images were reviewed by two radiologists in consensus and categorized according to American college of radiology breast imaging reporting and data system (ACR BI-RADS®) lexicon to make a final assessment.

### 3.4. 18F-FDG PET-CT

18F-FDG PET-CT imaging was performed using a Gemini TF (Philips medical systems, Cleveland, OH, USA). Normal fasting blood glucose levels (after fasting for at least 6 hours) were < 180 mg/dL for all patients. An intravenous

injection of 370 - 480 MBq (10 - 13 mCi) of FDG was administered according to body weight. Fifty minutes after the injection, pre-contrast CT scans were performed from the skull base to the upper thigh using the 16-channel scanner Brilliance 16 (Philips medical systems, Cleveland, OH, USA) with the following settings: 120 kVp; 50 mA; rotation time, 0.75 second; slice collimation, 0.75 mm; FOV, 60 cm; matrix, 512 × 512; and 4-mm scan reconstruction with a reconstruction index of 4 mm. These CT data were used for attenuation correction and anatomical correlation. Immediately after the CT scans, PET scans were performed for the same body region. PET acquisition data were reconstructed using the 3D Row Action Maximum Likelihood Algorithm and the CT scan data. The analysis of 18F-FDG PET-CT was done by experienced nuclear medicine physicians to determine abnormal FDG uptake in the breast parenchyma, chest wall, and axilla compared to that for normal tissue.

### 3.5. Pathological Examination

Diagnoses were made using specimens obtained from conserving operations or mastectomies. Histopathologic findings were reviewed by two experienced breast pathologists in consensus. The final tumor size, histological grade, presence of axillary lymph node metastasis, percentage of a ductal carcinoma in situ (DCIS) component, and the results of immunohistochemical tests for estrogen receptor (ER), progesterone receptor (PR), and human epidermal growth factor receptor 2 (HER2) were recorded. The statuses of ER and PR were evaluated according to the American society of clinical oncology/college of American pathologists (ASCO/CAP) guidelines for immunohistochemistry. ER and PR were considered positive if there were at least 1% positive tumor nuclei. HER2 immunostaining was read in a semi-quantitative manner and graded as follows: 0, 1+, 2+ and 3+. Intensity scores of 0 or 1+ were designated as negative expression, 2+ as equivocal expression, and 3+ as positive expression for HER-2/neu (10). Scores of 2+ were considered equivocal, and those samples were further recommended for fluorescent in situ hybridization (FISH) analysis (10). Specimens were also considered to be HER2-positive when they were shown to be positive by FISH (2).

## 4. Results

Of the twelve patients, ten patients were symptomatic, one patient had a tumor detected by screening, and one patient had a tumor detected incidentally on chest CT. The main symptom was a palpable mass or lump in the breast. One patient had a previous history of breast cancer and had undergone mastectomy and flap reconstruction

4 years before the new symptoms. The tumor involved the left breast in seven patients and the right breast in five patients.

Eleven patients had undergone pre-operative mammography. The breast parenchyma comprised scattered fibroglandular tissue in three patients, heterogeneously dense breast tissue in seven patients, and extremely dense breast tissue in one patient. No patients had almost entirely fatty breast tissue. Eight tumors resembled masses (Figures 1 and 2), two tumors resembled focal asymmetries, and one tumor resembled normal breast on mammography. The mammographic findings are shown in Table 1. According to the ACR BI-RADS lexicon, most mammograms were irregularly shaped (75%), indistinct margined masses (75%), and had equal density to the parenchyma (62.5%). None showed associated calcifications. Only one patient had enlarged axillary lymph nodes.

**Table 1.** The Mammographic Characteristics of ICC (n = 11)

Characteristics	No. (%)
<b>Occult</b>	1 (9.1)
<b>Focal asymmetry</b>	2 (18.2)
<b>Mass</b>	8 (72.7)
<b>Shape</b>	
Irregular	6 (75.0)
Round	2 (25.0)
<b>Margin</b>	
Indistinct	6 (75.0)
Spiculated	2 (25.0)
<b>Density</b>	
Equal density	5 (62.5)
High density	3 (37.5)
<b>Size</b>	
Mean (cm)	1.65
Range (cm)	1.1 - 2.2
<b>Associated microcalcification</b>	0
<b>Lymphadenopathy</b>	1 (9.1)

Values are expressed as number or percentage  
Abbreviation: ICC, invasive cribriform carcinoma.

Sonography was performed in all twelve patients, and all tumors presented as masses (Table 2). The most common sonographic findings of the masses were as follows: hypoechoogenicity (n = 12, 100%), irregular shape (n = 6, 50%), indistinct margins (n = 5, 41.7%), parallel orientation (n = 10, 83.3%), no posterior acoustic features (n = 10, 83.3%), and increased vascularity (n = 6, 50%).

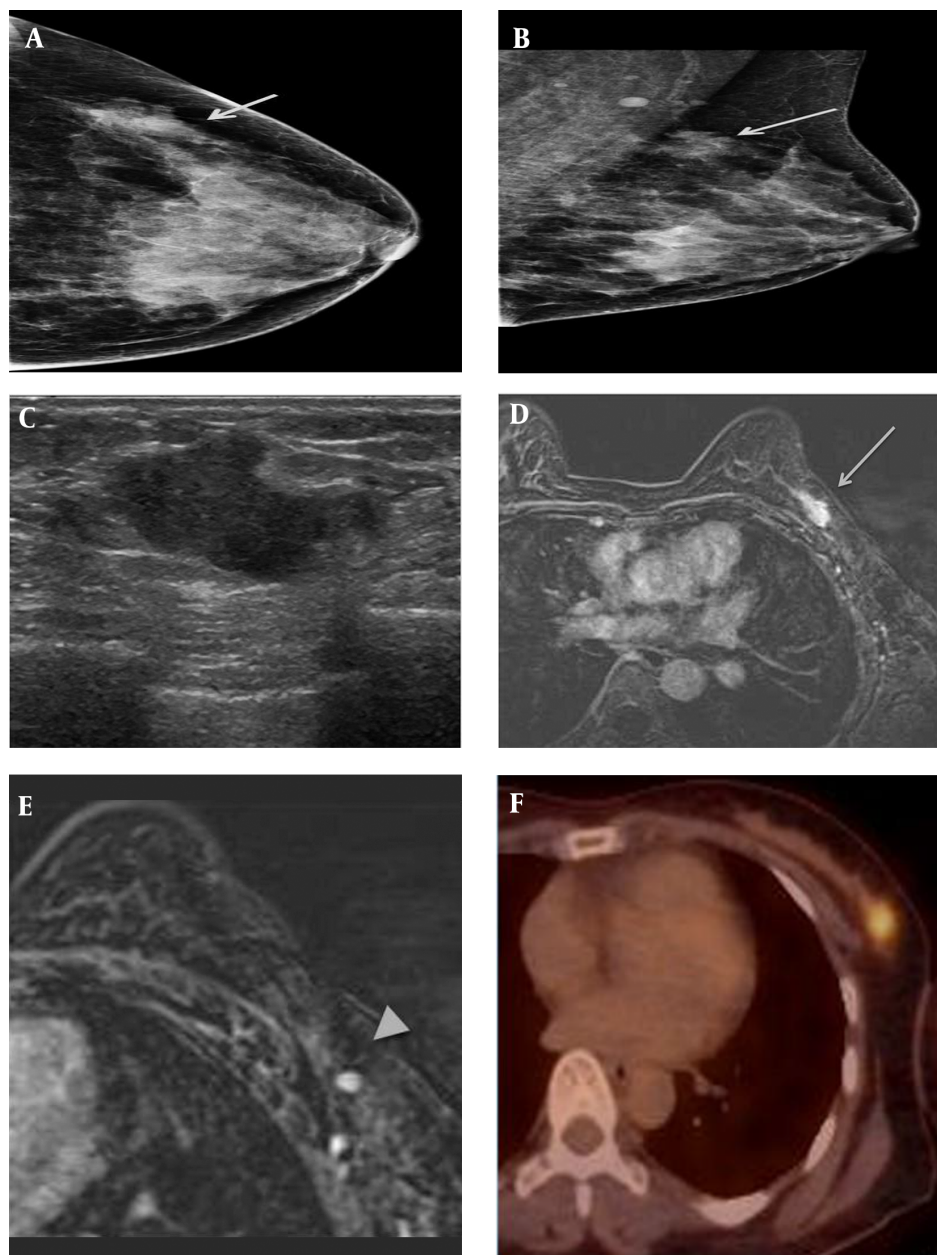


**Figure 1.** A 41-year-old female patient who presented with a palpable mass in the left breast. A and B, On mammography (A) craniocaudal (CC) view and (B) mediolateral oblique (MLO) view, an irregularly shaped, indistinct marginated isodense mass (solid arrow) was seen in the left upper outer quadrant, where the patient complained of a palpable mass. C, On sonography, an approximately 2.2-cm irregularly shaped, indistinct marginated hypoechoic mass was seen in the left breast in the 1 o'clock direction, 6 cm from the nipple. D&E, On axial fat-saturated T1-weighted 2-minute subtraction imaging, the mass (dashed arrow) was seen as an irregular marginated, oval-shaped mass with relatively homogeneous enhancement, measuring  $2.1 \times 1.1$  cm in size. There was also a small enhancing lymph node with cortical thickening in the ipsilateral axilla (arrowhead). F, on 18F-fluorodeoxyglucose positron emission tomography-computed tomography (18F-FDG PET-CT) the mass was seen as a focal hypermetabolic lesion.

All twelve patients also underwent pre-operative breast MRI and all presented as masses (Table 3). Nine patients had a single mass, and three patients had multiple masses (Figure 2). The shapes and margins of the masses were variable. Half of them were irregularly shaped, and

more than a half had irregular margins (66.7%). Most masses showed heterogeneous enhancement (75%) and type III kinetic patterns (75%) on dynamic studies. Only one patient had pectoralis muscle involvement, but that was the patient with a history of mastectomy.

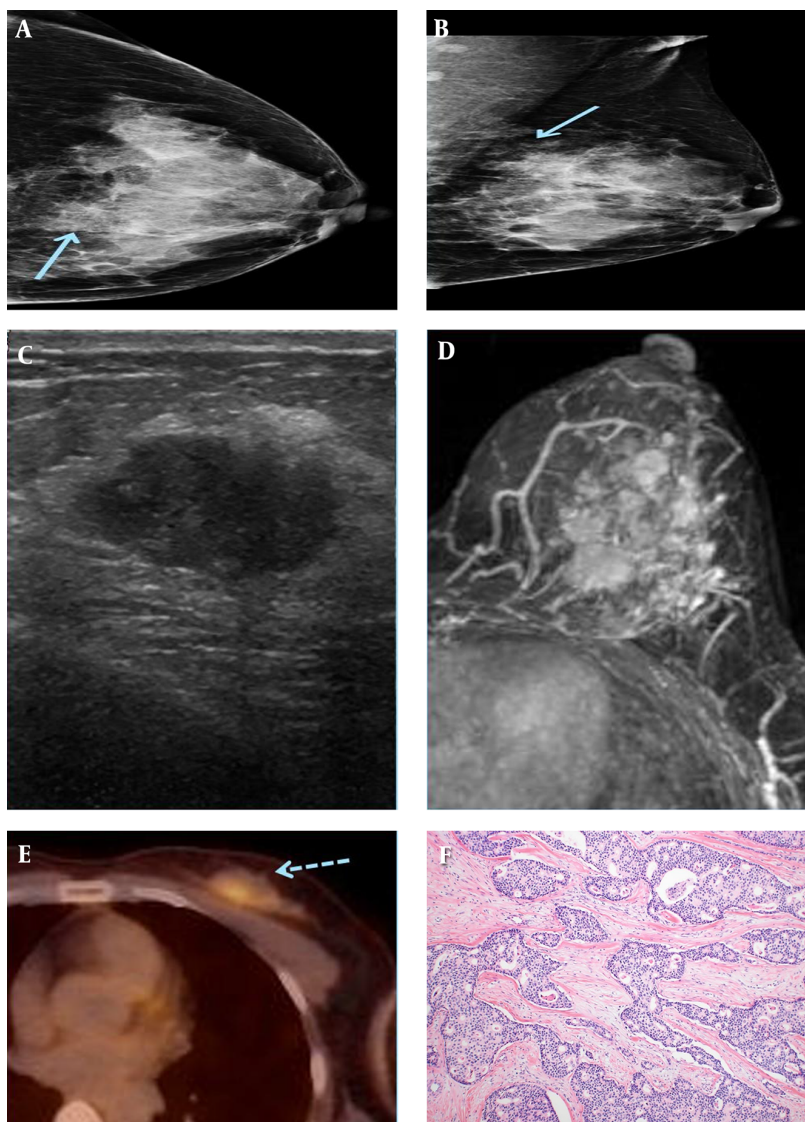


**Figure 2.** A 49-year-old female patient who presented with a palpable mass in the left breast. A and B, On mammography (A) craniocaudal (CC) view and (B) mediolateral-oblique (MLO) view, an irregularly shaped, indistinct marginated isodense mass (solid arrow) was seen in the left upper inner quadrant. C, An approximately 1.7-cm spiculated, oval-shaped hypoechoic mass was seen in the left breast in the 10 o'clock direction, 4 cm from the nipple on sonography. D, On axial fat-saturated T1-weighted 1-minute subtraction maximum intensity projection (MIP) imaging, multiple variably shaped masses with spiculated margins were seen, which all showed early rapid enhancement with delayed wash-out on dynamic study. E, These tumors exhibited increased FDG uptake (dashed arrow) on 18F-fluorodeoxyglucose positron emission tomography-computed tomography (18FFDG PET-CT). F, On microscopic examination (hematoxylin-eosin stain, original magnification x 100), the tumor is composed of cribriform or fenestrated cellular islands with smooth or angulated contouring. Extensive secondary lumen formation is observed, and some of the lumen is filled with eosinophilic secretion and occasional microcalcification. Unlike cribriform ductal carcinoma in situ (DCIS), desmoplastic stromal reaction is also observed in the background. The tumor cells show low grade of nuclear atypism and mitotic figures are rare. These cells have slightly enlarged nuclei with indistinct nucleoli.

18F-FDG PET-CT was performed in ten patients. All showed increased FDG uptake in the lesion, with markedly increased FDG uptake in nine patients (75.0%) and mild increased FDG uptake in one patient (8.3%). There were no distant metastases shown by 18F-FDG PET-CT.

The final pathologic diagnoses were obtained after breast conserving surgery in ten patients and mastectomy

in two patients. The final histopathologic diagnosis of all patients was pure invasive cribriform carcinoma. All, except one patient, had grade I tumors. Axillary lymph node metastases were identified in three patients. By immunohistochemistry, all patients were positive for ER and PR (n = 12, 100%) and negative for HER-2/neu (7 patients with score of 0 and 5 patients with score of 1+).

**Table 2.** The Sonographic Characteristics of ICC (n = 12)

Characteristics	No. (%)
<b>Shape</b>	
Irregular	6 (50.0)
Oval	4 (33.3)
Round	2 (16.7)
<b>Echogenicity</b>	
Low	12 (100.0)
<b>Orientation</b>	
Parallel	10 (83.3)
Non parallel	2 (16.7)
<b>Margin</b>	
Indistinct	5 (41.7)
Circumscribed	2 (16.7)
Microlobulated	2 (16.7)
Spiculated	2 (16.7)
Angular	1 (8.3)
<b>Posterior feature</b>	
None	10 (83.3)
Posterior enhancement	2 (16.7)
<b>Vascularity</b>	
Increased	6 (50.0)
Not increased	3 (25.0)
No Doppler study	3 (25.0)
<b>Size</b>	
Mean	1.76
Range	0.9 - 2.7
Lymphadenopathy	1 (8.3)

Values are expressed as number or percentage  
Abbreviation: ICC, invasive cribriform carcinoma.

**Table 3.** The MRI Findings of ICC (n = 12)

Characteristics	No. (%)
<b>Morphology</b>	
Mass	12 (100.0)
<b>Multiplicity</b>	
Single	9 (75.0)
Multiple	3 (25.0)
<b>Shape</b>	
Irregular	6 (50.0)
Oval	4 (33.3)
Round	2 (16.7)
<b>Margin</b>	
Irregular	8 (66.7)
Smooth	3 (25.0)
Spiculated	1 (8.3)
<b>Enhancement pattern</b>	
Heterogeneous	9 (75.0)
Rim	2 (16.7)
Homogeneous	1 (8.3)
<b>Kinetics</b>	
Type I	9 (75.0)
Type II	0
Type III	3 (25.0)
<b>Size</b>	
Mean (cm)	1.78
Range (cm)	0.7 - 2.3
<b>Lymphadenopathy</b>	4 (33.3)
<b>Pectoralis invasion</b>	1 (8.3)

Values are expressed as number or percentage  
Abbreviations ICC, invasive cribriform carcinoma.

## 5. Discussion

ICC is a rare type of invasive ductal carcinoma of the breast, with an incidence of about 0.3% - 6% of primary breast cancers (5, 6, 11). In our institution, twelve cases of ICC were diagnosed while 3242 cases of invasive carcinomas and 857 cases of ductal carcinoma in situ of the breast were diagnosed in the same period of time. Thus, the percentage of ICC to invasive carcinoma of the breast was about 0.37% in this study.

ICC is defined histologically by a predominant cribriform growth pattern, which is observed as cells arranged in sheets of trabeculae with distinctive empty luminal spaces, in its invasive component (2, 5, 7). The cytologi-

cal features typically seen in ICC are small cell size, amphophilic cytoplasm, indistinct cell boundaries, small to medium-sized nuclei with a sharp nuclear membrane, and finely stippled chromatin (6). ICC usually exhibits a high degree of differentiation with low or moderate nuclear grade (6). There are two types of ICC: classic, which is also termed pure, and mixed (5, 6, 11). The pure type has invasive cribriform architecture almost entirely (at least 90%) with or without less than 50% of tubular pattern (5, 6). Mixed ICC has more than 50% of cribriform pattern in the invasive components, with the remainder composed of a less well-differentiated pattern (5, 6). Pure ICC is very rare and is known to be associated with smaller size, less lymph

node involvement, lower tumor stage, and better prognosis, compared with mixed ICC (2, 5).

ICC imaging findings are not well known since there have only been a few studies describing this tumor, and the incidence of the tumor is very low. There are several studies that report the radiologic findings of ICC on mammography and sonography. Stutz et al. (12) reported that ICC manifests as a large spiculated mass with or without punctate calcifications on mammography. Nishimura et al. (13) reported a case of ICC that developed in a male patient presenting with a circumscribed hyperdense mass with extensive microcalcifications on mammography. In the study conducted by Cong et al. (4), six out of eight tumors were seen as hyperdense masses on mammography without visible microcalcifications. Another study of 28 cases of ICC reported that most lesions presented with irregular shapes and spiculated margins on mammography. One-thirds of patient tumors had microcalcifications on mammography, and more than three-quarters of patient tumors contained associated DCIS components. However, there was no significant relationship between the DCIS component and the microcalcifications (14). In our study, about 70% of the tumors were seen as a mass on mammography. The most common characteristics of the masses were irregular shapes, indistinct margins, and equal densities. There was no case with calcification.

On sonography, all tumors appeared as hypoechoic masses, with variable shapes and margins in this study. The most common characteristics were irregular shapes and indistinct margins, which are typical sonographic findings of breast malignancies. All tumors lacked posterior features, except two that exhibited posterior acoustic enhancement. This result follows those of previous studies, which showed that most lesions appeared as hypoechoic masses with the majority having irregular shapes (4, 12, 14, 15). There was a discrepancy in the descriptions of tumor margins, being partially microlobulated, well-defined, ill-defined, or spiculated (4, 12, 14, 15). According to Stutz et al. (12), the majority of tumors did not have posterior acoustic enhancement, which contrasts with other forms of breast cancer, in which posterior acoustic attenuation is found in most tumors (16). There are several publications that report sonographic findings according to the histological grade of breast cancer suggesting that the margins the margins seen on radiologic studies may reflect the histological grades of the tumor (10, 11, 17, 18). According to these studies, tumors with low histologic grades are more likely to have indistinct or spiculated margins, owing to the low degree of desmoplastic reactions, while tumors with high grades tend to have microlobulated margins and posterior acoustic enhancement. Supporting those reports, most masses in our study had spiculated or indistinct margins

on mammography and sonography, and all tumors were confirmed low histologic grade (grade I).

There are very limited data about the MRI appearance of ICC. Lee et al. (14) reported that the most common MRI characteristic of ICC is irregularity. They also reported that about 16.0% of tumors presented as a non-mass-like enhancement with segmental distribution on MRI, which might be primarily due to the DCIS component. A case report of ICC described the MRI appearance of the mass as an oval-shaped, smooth margined mass with early fast enhancement and a delayed kinetic wash-out pattern (19). This type III kinetic pattern has been also reported in a study by Lim et al. (15). In our study, all 12 tumors were seen as a mass, with 9 single and 3 multiple masses. Most masses had irregular margins (66.7%) and irregular shapes (50.0%) with heterogeneous enhancement (83.3%). By dynamic study, all but three lesions showed early fast enhancement and delayed wash-out patterns.

There is only one study for 18F-FDG PET-CT image findings of ICCs, which reported that increased FDG uptake was seen in the majority (87%) of the tumors (14). This result correlates with that of our study, in which about 83% of tumors exhibited increased FDG uptake. Although PET-CT is not recommended for routine staging of breast cancer at this time, it may provide additional information on breast cancer staging, especially when the results of conventional imaging are ambiguous or conflicting (18, 20-23).

The presence of cribriform components in a tumor is associated with a good prognosis. Previous studies suggest that pure ICC has a relatively favorable prognosis and a low frequency of lymph node metastases (5-7). Page et al. (5) reported a 100% 10-year survival for patients with pure ICC, and Venable et al. (6) and Ellis et al. (7) also supported this result with similar conclusions suggesting a 10-year survival rate of more than 90%. In our study, ICC was associated with several factors indicating favorable prognosis, such as small tumor size, low tumor grade, low frequency of axillary lymph node metastasis (25%), positive ER and PR expression (100%), and negative HER-2/neu expression (100%). As in the present cases, ICCs usually had low or moderate nuclear grades, positive ER and PR expression, and rare HER-2 amplification in many previous studies (4, 6, 8, 24). These findings are probably due to ICC being a well-differentiated neoplasm architecturally, cytologically, ultrastructurally, and functionally (24). These factors could contribute to the excellent prognoses of patients with pure ICC (4, 5, 14).

This study has several limitations. First, this is a retrospective study which not all patients through all imaging modalities: mammography, sonography, MRI, and 18F-FDG PET-CT. Secondly, the sample size was small, and thus generalizing the findings reported in this study should be done

with caution. However, this is due to the scarcity of ICC. Thirdly, this study is from a single institution of a tertiary referral center, which may limit the generalizability due to the use of the latest equipment and the availability of expert readers evaluating the lesions.

In conclusion, invasive cribriform carcinomas (ICCs) of the breast appear as masses with typical features of malignancy on mammography, sonography, MRI, and 18F-FDG PET-CT. ICC usually presented without associated calcifications and showed rare spiculation, unlike invasive ductal carcinoma of no special type, the most common invasive breast malignancy.

## Footnotes

**Authors' Contributions:** Study concept and design: Youyeon Kim, and Kyu Ran Cho; acquisition of data: Youyeon Kim, and Kyu Ran Cho; analysis and interpretation of data: Youyeon Kim, Kyu Ran Cho, and Jeong Hyun Lee; drafting of the manuscript: Youyeon Kim; critical revision of the manuscript for important intellectual content: Kyu Ran Cho, Bo Kyoung Seo, and Ok Hee Woo; administrative, technical, and material support: Sung Eun Song, and Sung Bum Cho; study supervision: Kyu Ran Cho, and Sung Bum Cho.

**Financial Disclosure:** This original research did not receive commercial financial support and the authors have no conflicts of interest.

**Funding/Support:** This work did not receive commercial financial support.

## References

- International agency for research on cancer . GLOBOCAN 2012 : Estimated Cancer incidence, mortality and prevalence worldwide in 2012. World Health Organization 2015. Available from: <http://globocan.iarc.fr>.
- Lakhani SR. WHO classification of tumours of the breast. International Agency for Research on Cancer; 2012.
- Sinn HP, Kreipe H. A Brief Overview of the WHO Classification of Breast Tumors, 4th Edition, Focusing on Issues and Updates from the 3rd Edition. *Breast Care (Basel)*. 2013;**8**(2):149–54. doi: [10.1159/000350774](https://doi.org/10.1159/000350774). [PubMed: [24415964](https://pubmed.ncbi.nlm.nih.gov/24415964/)].
- Cong Y, Qiao G, Zou H, Lin J, Wang X, Li X, et al. Invasive cribriform carcinoma of the breast: A report of nine cases and a review of the literature. *Oncol Lett*. 2015;**9**(4):1753–8. doi: [10.3892/ol.2015.2972](https://doi.org/10.3892/ol.2015.2972). [PubMed: [25789036](https://pubmed.ncbi.nlm.nih.gov/25789036/)].
- Page DL, Dixon JM, Anderson TJ, Lee D, Stewart HJ. Invasive cribriform carcinoma of the breast. *Histopathology*. 1983;**7**(4):525–36. [PubMed: [6884999](https://pubmed.ncbi.nlm.nih.gov/6884999/)].
- Venable JG, Schwartz AM, Silverberg SG. Infiltrating cribriform carcinoma of the breast: a distinctive clinicopathologic entity. *Hum Pathol*. 1990;**21**(3):333–8. [PubMed: [2312110](https://pubmed.ncbi.nlm.nih.gov/2312110/)].
- Ellis IO, Galea M, Broughton N, Locker A, Blamey RW, Elston CW. Pathological prognostic factors in breast cancer. II. Histological type. Relationship with survival in a large study with long-term follow-up. *Histopathology*. 1992;**20**(6):479–89. [PubMed: [1607149](https://pubmed.ncbi.nlm.nih.gov/1607149/)].
- Zhang W, Zhang T, Lin Z, Zhang X, Liu F, Wang Y, et al. Invasive cribriform carcinoma in a Chinese population: comparison with low-grade invasive ductal carcinoma-not otherwise specified. *Int J Clin Exp Pathol*. 2013;**6**(3):445–57. [PubMed: [23412348](https://pubmed.ncbi.nlm.nih.gov/23412348/)].
- Elverici E, Zengin B, Nurdan Barca A, Didem Yilmaz P, Alimli A, Araz L. Interobserver and Intraobserver Agreement of Sonographic BIRADS Lexicon in the Assessment of Breast Masses. *Iran J Radiol*. 2013;**10**(3):122–7. doi: [10.5812/iranjradiol.10708](https://doi.org/10.5812/iranjradiol.10708). [PubMed: [24348596](https://pubmed.ncbi.nlm.nih.gov/24348596/)].
- Goud KI, Dayakar S, Vijayalaxmi K, Babu SJ, Reddy PV. Evaluation of HER-2/neu status in breast cancer specimens using immunohistochemistry (IHC) & fluorescence in-situ hybridization (FISH) assay. *Indian J Med Res*. 2012;**135**:312–7. [PubMed: [22561616](https://pubmed.ncbi.nlm.nih.gov/22561616/)].
- Marzullo F, Zito FA, Marzullo A, Labriola A, Schittulli F, Gargano G, et al. Infiltrating cribriform carcinoma of the breast. A clinic-pathologic and immunohistochemical study of 5 cases. *Eur J Gynaecol Oncol*. 1996;**17**(3):228–31. [PubMed: [8780923](https://pubmed.ncbi.nlm.nih.gov/8780923/)].
- Stutz JA, Evans AJ, Pinder S, Ellis IO, Yeoman LJ, Wilson AR, et al. The radiological appearances of invasive cribriform carcinoma of the breast. Nottingham Breast Team. *Clin Radiol*. 1994;**49**(10):693–5. [PubMed: [7955831](https://pubmed.ncbi.nlm.nih.gov/7955831/)].
- Nishimura R, Ohsumi S, Teramoto N, Yamakawa T, Saeki T, Takashima S. Invasive cribriform carcinoma with extensive microcalcifications in the male breast. *Breast Cancer*. 2005;**12**(2):145–8. [PubMed: [15858447](https://pubmed.ncbi.nlm.nih.gov/15858447/)].
- Lee YJ, Choi BB, Suh KS. Invasive cribriform carcinoma of the breast: mammographic, sonographic, MRI, and 18 F-FDG PET-CT features. *Acta Radiol*. 2015;**56**(6):644–51. doi: [10.1177/0284185114538425](https://doi.org/10.1177/0284185114538425). [PubMed: [24938660](https://pubmed.ncbi.nlm.nih.gov/24938660/)].
- Lim HS, Jeong SJ, Lee JS, Park MH, Yoon JH, Kim JW, et al. Sonographic findings of invasive cribriform carcinoma of the breast. *J Ultrasound Med*. 2011;**30**(5):701–5. [PubMed: [21527619](https://pubmed.ncbi.nlm.nih.gov/21527619/)].
- Jackson VP. Sonography of malignant breast disease. *Semin Ultrasound CT MR*. 1989;**10**(2):119–31. [PubMed: [2697327](https://pubmed.ncbi.nlm.nih.gov/2697327/)].
- Lamb PM, Perry NM, Vinnicombe SJ, Wells CA. Correlation between ultrasound characteristics, mammographic findings and histological grade in patients with invasive ductal carcinoma of the breast. *Clin Radiol*. 2000;**55**(1):40–4. doi: [10.1053/crad.1999.0333](https://doi.org/10.1053/crad.1999.0333). [PubMed: [10650109](https://pubmed.ncbi.nlm.nih.gov/10650109/)].
- Gil-Rendo A, Martinez-Regueira F, Zornoza G, Garcia-Velloso M, Beorlegui C, Rodriguez-Spiteri N. Association between [18F]fluorodeoxyglucose uptake and prognostic parameters in breast cancer. *Br J Surg*. 2009;**96**(2):166–70. doi: [10.1002/bjs.6459](https://doi.org/10.1002/bjs.6459). [PubMed: [19160365](https://pubmed.ncbi.nlm.nih.gov/19160365/)].
- Heo TW, L IH, Lee JS, Park MH, Jeong SJ. Invasive cribriform carcinoma of the breast: A case report. *J Korean Soc Radiol*. 2011;**64**(1):83–6.
- Rosen EL, Eubank WB, Mankoff DA. FDG PET, PET/CT, and breast cancer imaging. *Radiographics*. 2007;**27** Suppl 1:S215–29. doi: [10.1148/rg.27si075517](https://doi.org/10.1148/rg.27si075517). [PubMed: [18180228](https://pubmed.ncbi.nlm.nih.gov/18180228/)].
- De Cicco C, Gilardi L, Botteri E, Fracassi SL, Di Dia GA, Botta F, et al. Is [18F] fluorodeoxyglucose uptake by the primary tumor a prognostic factor in breast cancer? *Breast*. 2013;**22**(1):39–43. doi: [10.1016/j.breast.2012.05.009](https://doi.org/10.1016/j.breast.2012.05.009). [PubMed: [22704459](https://pubmed.ncbi.nlm.nih.gov/22704459/)].
- Ergul N, Kadioglu H, Yildiz S, Yucel SB, Gucin Z, Erdogan EB, et al. Assessment of multifocality and axillary nodal involvement in early-stage breast cancer patients using 18F-FDG PET/CT compared to contrast-enhanced and diffusion-weighted magnetic resonance imaging and sentinel node biopsy. *Acta Radiol*. 2015;**56**(8):917–23. doi: [10.1177/0284185114539786](https://doi.org/10.1177/0284185114539786). [PubMed: [25013091](https://pubmed.ncbi.nlm.nih.gov/25013091/)].
- Furukawa H, Ikuma H, Asakura K, Uesaka K. Prognostic importance of standardized uptake value on F-18 fluorodeoxyglucose-positron emission tomography in biliary tract carcinoma. *J Surg Oncol*. 2009;**100**(6):494–9. doi: [10.1002/jso.21356](https://doi.org/10.1002/jso.21356). [PubMed: [19653260](https://pubmed.ncbi.nlm.nih.gov/19653260/)].
- Wells CA, Ferguson DJ. Ultrastructural and immunocytochemical study of a case of invasive cribriform breast carcinoma. *J Clin Pathol*. 1988;**41**(1):17–20. [PubMed: [3343375](https://pubmed.ncbi.nlm.nih.gov/3343375/)].